Development 139, 699-708 (2012) doi:10.1242/dev.068791

Synchronous and symmetric migration of *Drosophila* caudal visceral mesoderm cells requires dual input by two FGF ligands

Snehalata Kadam, Srimoyee Ghosh and Angelike Stathopoulos*

SUMMARY

Caudal visceral mesoderm (CVM) cells migrate synchronously towards the anterior of the *Drosophila* embryo as two distinct groups located on each side of the body, in order to specify longitudinal muscles that ensheath the gut. Little is known about the molecular cues that guide cells along this path, the longest migration of embryogenesis, except that they closely associate with trunk visceral mesoderm (TVM). The expression of the fibroblast growth factor receptor (FGFR) *heartless* and its ligands, *pyramus* (*pyr*) and *thisbe* (*ths*), within CVM and TVM cells, respectively, suggested FGF signaling may influence CVM cell guidance. In FGF mutants, CVM cells die before reaching the anterior region of the TVM. However, an earlier phenotype observed was that the two cell clusters lose direction and converge at the midline. Live in vivo imaging and tracking analyses identified that the movements of CVM cells were slower and no longer synchronous. Moreover, CVM cells were found to cross over from one group to the other, disrupting bilateral symmetry, whereas such mixing was never observed in wild-type embryos. Ectopic expression of either Pyr or Ths was sufficient to redirect CVM cell movement, but only when the endogenous source of these ligands was absent. Collectively, our results show that FGF signaling regulates directional movement of CVM cells and that native presentation of both FGF ligands together is most effective at attracting cells. This study also has general implications, as it suggests that the activity supported by two FGF ligands in concert differs from their activities in isolation.

KEY WORDS: Cell migration, FGF signaling, Longitudinal visceral mesoderm precursor cells, Caudal visceral mesoderm, *Drosophila* embryogenesis

INTRODUCTION

Cell migration is a fundamental process during embryonic development that involves interplay between extracellular signaling molecules, cell surface receptors and intracellular signal transduction pathways (reviewed by Aman and Piotrowski, 2010; Keller, 2005; Kunwar et al., 2006; Ridley et al., 2003). Movement of cells is often directional, with cells sensing the appropriate direction of migration based on recognition of region-specific cues (Parent and Devreotes, 1999; Rorth, 2011). Collective cell migration must be regulated temporally and spatially for organisms to develop properly, and can play an important role in homeostatic processes such as the immune response and the repair of injured tissues (Friedl and Gilmour, 2009; Montell, 2006).

In *Drosophila*, caudal visceral mesoderm (CVM) cells, the founders of longitudinal visceral muscles, originate from the posterior end of the embryonic mesoderm and subsequently undergo the longest cell migration of *Drosophila* embryogenesis (Fig. 1A-D) (Georgias et al., 1997; Kusch and Reuter, 1999). Migration is a necessary step for their specification into longitudinal muscle fibers. Little is known about the molecular guidance cues that support this migration process. However, in mutants that eliminate function of the fibroblast growth factor receptor (FGFR) Heartless (Htl), it was found that longitudinal visceral muscle fibers are absent, and one proposed explanation was that Htl may play a role in supporting CVM cell survival (Mandal et al., 2004).

Division of Biology, California Institute of Technology, 1200 East California Boulevard, MC114-96, Pasadena, CA 91125, USA.

*Author for correspondence (angelike@caltech.edu)

Accepted 30 November 2011

In *Drosophila*, FGF signaling through the Htl FGFR plays multiple roles in mesoderm development (Beiman et al., 1996; Gisselbrecht et al., 1996; Michelson et al., 1998). During gastrulation, Htl FGFR-activation by either FGF ligands Pyramus (Pyr) or Thisbe (Ths) supports distinct as well as overlapping activities: Ths controls collapse of the invaginated mesodermal tube; both ligands are required to form a cell monolayer at the culmination of mesoderm spreading; and, following mesoderm spreading, Pyr predominantly supports differentiation of dorsal mesoderm lineages (Klingseisen et al., 2009; McMahon et al., 2010; Michelson et al., 1998). It does not appear that dedicated functions can be ascribed to a ligand for the course of development. For example, Thisbe supports mesoderm cell movement in the early embryo (Klingseisen et al., 2009; McMahon et al., 2010), but supports cell differentiation in the eye (Franzdottir et al., 2009). Therefore, ligand functions are probably context dependent.

It is also not known whether Pyr and Ths ligands activate the Htl FGFR individually as homodimers or coordinately as heterodimers, and this is also an unresolved issue in the FGF field. Although studies in vertebrate systems postulate that heterodimeric FGF ligand combinations do activate FGFRs and structural studies of FGF-FGFR interactions support this view (Plotnikov et al., 2000; Zhang et al., 2006), to our knowledge, no definitive experimental evidence exists. Over 120 FGF-FGFR interactions are presumed to function in vertebrates (Zhang et al., 2006), whereas evidence for activity of three combinations has been presented in *Drosophila* (Kadam et al., 2009; Tulin and Stathopoulos, 2010). Here, taking advantage of this simplified receptor-ligand system in *Drosophila*, we studied the differential effects of multiple FGF ligands in activating the same FGFR receptor and how this contributes to symmetric and synchronous migration of CVM cells.

MATERIALS AND METHODS

Drosophila fly stocks and genetics

All crosses and strains were maintained at 25°C. The following lines were used: *yw*, *croc-lacZ* (Hacker et al., 1995) and *UAS-CD2 G447.Gal4* (Georgias et al., 1997) for wild type; *DfBSC25*/*CyO wg-lacZ* (CWLZ) (Stathopoulos et al., 2004), *Df(2R)ths238*/CWLZ (Kadam et al., 2009), *Df(2R)pyr36*/CWLZ (Kadam et al., 2009) and htl^{AB42}/*TM3 ftz-lacZ* (TFLZ) (Gisselbrecht et al., 1996).

The Gal4 driver *sim.Gal4* was obtained from Stephen Crews (University of North Carolina, Chapel Hill, NC, USA) (Xiao et al., 1996), *bap.Gal4* from Manfred Frasch (University of Erlangen-Nuremberg), *fkh.Gal4* from Deborah Andrew (Johns Hopkins University School of Medicine, Baltimore, MD, USA) (Henderson and Andrew, 2000), *UAS.p35* from the Bloomington Stock Center, *UAS.DN-Htl* from Alan Michelson (Harvard Medical School, Boston, Massachusetts), *UAS.htl-RNAi* (40627) from VDRS stock center (Vienna, Austria) and ush^{HOA27}/CyO from Rolf Reuter (University of Tuebingen, Germany). *UAS.pyr* (AMS330-3) and *UAS.ths* (AMS289-22) stocks, described previously (Kadam et al., 2009), were recombined with the bHLH54F-H2A.mCherry reporter generated in this study.

The following fly stocks were created using standard genetic crosses:

(1) DfBSC25/CWLZ; UAS.p35, (2) bap.Gal4; DfBSC25/CWLZ, (3) DfBSC25/CWLZ; fkh.Gal4/TFLZ, (4) DfBSC25 UAS.CD2 G447.Gal4/CWLZ, (5) DfBSC25 sim.Gal4/CWLZ, (6) DfBSC25 sim.Gal4/CWLZ; UAS.ths, (7) DfBSC25 sim.Gal4/CWLZ; UAS.pyr/TFLZ, (8) DfBSC25 croc.lacZ/CWLZ; UAS.ths and (9) DfBSC25 croc.lacZ/CWLZ; UAS.pyr.

CyO wg.lacZ (CWLZ) balancers were used in staining experiments and CyO dfd-GMR-Venus (CDV) (Lee et al., 2006) were used for imaging studies, whenever possible.

Fixation, immunohistochemistry and in situ hybridization

Embryos were fixed and stained using in situ, antibody, or combined antibody and in situ protocols as previously described (Jiang et al., 1991; Kosman et al., 2004). The following antibodies were used in the study: rabbit anti-β-gal antibody (1:400; Molecular Probes), mouse anti-Fas III antibody (1:10; Developmental Studies Hybridoma Bank), mouse anti-CD2 antibody (1:300; Serotec), mouse anti-bio (1:500; Roche) and sheep anti-dig (1:500; Roche). Embryos were mounted in Permount (Fischer Scientific) for whole-mount studies or embedded in acetone-araldite (Electron Microscopy Sciences) and cut with a microtome (LKB Bromna) to create 10 μm sections. Fluorescently labeled embryos were mounted in Vecta-shield mounting medium (Vector Laboratories) and images were obtained with a Pascal confocal microscope (Carl Zeiss).

TUNEL assays were carried out using the Millipore Apoptag Peroxidase InSitu Apoptosis Detection Kit as previously described (Reim et al., 2003) with the modification of Proteinase K treatment for 1 minute.

Construction of fluorescent reporter for live in vivo imaging of CVM migration

To construct a fluorescent reporter, we used a CVM-specific enhancer associated with the *bHLH54F* gene (Ismat et al., 2010) to support expression of nuclearly localized mCherry fluorescent protein within the CVM cells. DNA (1.5 kb) was isolated from the entire second intron of the bHLH54F gene using PCR, based on ChIP-chip binding data in this region for the visceral mesoderm-associated transcription factor Biniou (Jakobsen et al., 2007). This sequence was placed upstream of the *even-skipped* minimal promoter driving expression of a reporter gene, Histone2A (H2A) fused to mCherry (bHLH.H2A-mCherry). Transgenic stocks were isolated using standard P-element transgenesis.

Genetic backgrounds of embryos used for live imaging

For rescue experiment movies: *DfBSC25* sim.Gal4/CDV was crossed with *DfBSC25*/CDV; UASths bHLH.H2A-mCherry to obtain 1×ths rescue movies. For 2×ths movies, *DfBSC25* sim.Gal4/CWLZ; UAS.ths/UAS.ths (chr III homozygous viable) stock was crossed with *DfBSC25*/CDV; UAS.ths bHLH.H2A-mCherry. For 1×pyr movies, *DfBSC25* sim.Gal4/CDV was crossed with DfBSC25/CDV; UAS.pyr bHLH.H2A-mCherry. For 2×pyr movies, *DfBSC25*, sim.Gal4/CWLZ; UAS.pyr/TFLZ (chromosome III homozygous lethal) was crossed to *DfBSC25*/CDV; UAS.pyr bHLH.H2A-mCherry. For 1×pyr+1×ths movies, *DfBSC25* sim.Gal4/CWLZ; UAS.ths was crossed to *DfBSC25*/CDV; UAS.pyr bHLH.H2A-mCherry.

Stocks *DfBSC25* sim.Gal4/CWLZ; UAS.ths and *DfBSC25* sim.Gal4/CWLZ; UAS.pyr/TFLZ could not be rebalanced using drd-Venus balancers because such lines were not viable; presumably, genetic interactions prevented their generation. Therefore, for isolation of 2×ths and 2×pyr rescue experiments in the *DfBSC25* background, we relied on viability assay to distinguish homozygotes from heterozygotes (i.e. *DfBSC25* homozygous mutants died by stage 16-17, whereas heterozygotes were viable). Head malformation defects associated with the *DfBSC25* homozygous mutant background served as secondary confirmation of genotype. In addition, for 2×pyr, we could not homozygose UAS.pyr on chromosome III as it was lethal in combination with sim.Gal4. Therefore, we imaged nine *DfBSC25* homozygous embryos, of which half were expected to contain 2×pyr.

As controls, *DfBSC25 sim.Gal4*/CWLZ; UAS.ths and *DfBSC25* sim.Gal4/CDV lines were crossed with UAS.pyr bHLH.H2A-mCherry (chromosome III homozygous viable in a wild-type background). All embryos ectopically expressed *pyr* at the midline and yet no CVM cell migration phenotypes were observed. Furthermore, all imaged embryos were viable (n=5).

Live imaging and image analysis

For live imaging, staged embryos were dechorionated using 50% bleach (Sigma) for 30 seconds. Stage 10 embryos were manually picked from a dark background agar plate using a light microscope. The selected dorsally or laterally oriented embryos were mounted on a heptane glue slide, and a drop of water was placed on the embryos to maintain their survival during imaging.

Embryos were imaged using a Zeiss Pascal confocal microscope at 543 nm wavelength with a 40× water lens. The specifications for live imaging are as follows: laser power, 25% or 0.25 mW; pixel time, 12.69 μseconds; pinhole, 8.77 AU; total time interval between start of one scan to another, 3.3 minutes; z-stack size, 57.28 μm; z-stack overlap, 9.55 μm. The specifications for movies that were used for tracking are as follows: laser power, 30% or 0.3 mW; pixel time, 3.20 μseconds; pinhole, 7.43 AU; time interval, 2 minutes and 34 seconds; z-stack size, 60.06 μm; z-stack overlap, 7.2 μm.

For the cell-tracking study, we analyzed the following movies: three embryos of wild-type bHLH.H2A-mCherry and *Df(2R)BSC25*/CDV; bHLH.H2A-mCherry backgrounds; two embryos of *DfBSC25* G447.Gal4/CWLZ × *DfBSC25*/CWLZ;UAS.pyr bHLH.H2A-mCherry background; and one embryo from the htl^{AB42} bHLH.H2A-mCherry/TM3-dfd-GMR-Venus YFP (TDV) background. All the embryos used for making of movies were followed until hatching to confirm viability in case of heterozygotes and lethality in the case of homozygotes. Imaris software (Bitplane) was used to perform tracking on imaged data. Individual cells were manually tracked by following their nuclei throughout the course of 3.5 hours. Time '0' corresponds roughly to the separation of CVM cells into two cell groups on either side of the embryo (i.e. left and right), unless otherwise noted.

RESULTS

CVM cell movement involves active migration of cells

We used a previously characterized *croc-lacZ* reporter gene to visualize CVM cells throughout the course of their migration (see Fig. 1E-H compare with 1A-D) (Hacker et al., 1995). Two bilaterally symmetric clusters of cells form at stage 10 and migrate toward the anterior in a synchronous fashion (supplementary material Fig. S1D-F). The extent of CVM cell migration correlates precisely with developmental stage (supplementary material Fig. S1A-C). At the end of the migration, CVM cells specify longitudinal muscles that ensheath the gut.

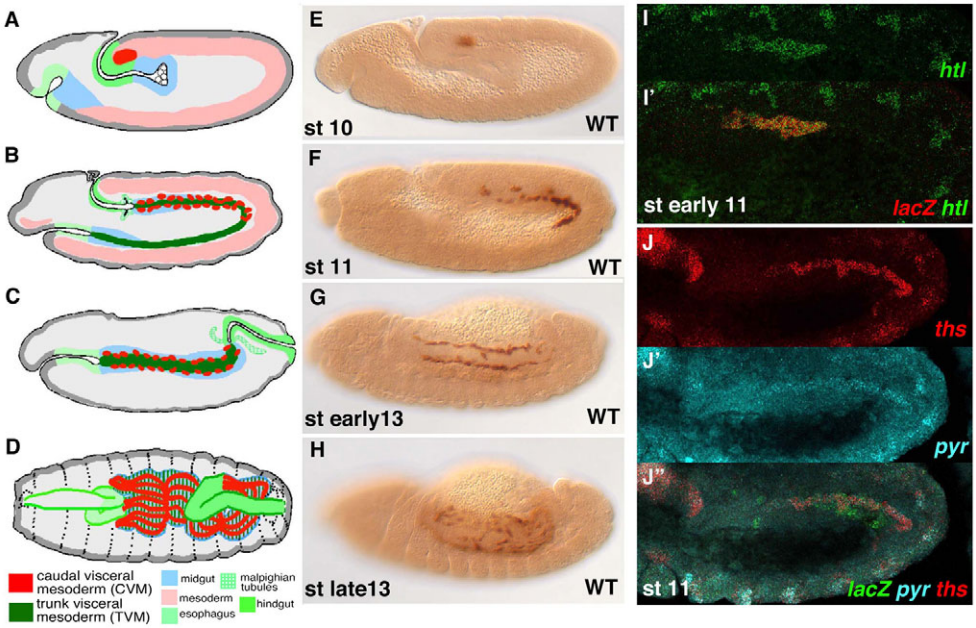

Fig. 1. FGF ligands *pyramus* and *thisbe* are expressed in the TVM, and the FGF receptor *heartless* is expressed in migrating CVM cells. Embryos are oriented with anterior towards the left and dorsal upwards. (**A-D**) Schematic representation of visceral mesoderm and endoderm development. (A) At stage 10, CVM cells (red) originate as a single group of cells arising from the posterior tip of the mesoderm anlage. (B) At stage 11, CVM cells arrange themselves in two rows on either side of the midgut primordium and subsequently migrate anteriorly along the TVM. (C,D) At stage 13, the CVM cells reach their final destination along the TVM (C) and adopt the elongated morphology characteristic of longitudinal muscle fibers (D). Adapted from an image kindly provided by R. Reuter (University of Tuebingen, Germany). (**E-H**) Anti-βgal antibody staining of wild-type embryos containing the *croc-lacZ* reporter gene depicting the steps of migratory CVM cell development at stages equivalent to schematics in A-D. (**I-J″**) Embryos expressing *croc.lacZ* stained using riboprobes to *htl, pyr, ths* and/or *lacZ* by multiplex fluorescent in situ hybridization. (I-I′) *htl* (green) and *lacZ* (red) colocalize within migrating CVM cells. (J-J″) *ths* (red) and *pyr* (blue) expression detected within the TVM, and *lacZ* (green) expression detected within migrating CVM cells.

As germ band retraction (GBR) occurs at stage 11 after CVM cells have initiated migration but before its completion (supplementary material Fig. S1F), we investigated whether any part of CVM cell migration might passively reflect movement of these cells resulting from GBR. We assayed CVM migration within *u-shaped* (*ush*) mutants, in which GBR does not occur (Goldman-Levi et al., 1996), and found that CVM cells continue to migrate toward the anterior (supplementary material Fig. S1G). This result suggested that active migration is likely to be required for cells to reach the anterior.

CVM migration is aberrant in the absence of either the Htl FGFR or Pyr and Ths FGF ligands

As the CVM cells migrate from the posterior of the embryo to the anterior, each group of migrating CVM cells remains closely associated with one of the two bands of TVM tissue present on either side of the embryonic body, especially from stage 11 onwards (Fig. 2A-C, left side view). This observation suggested to us that the TVM might support guidance of CVM cell migration, and our previous study had identified that the FGF ligand *thisbe* is expressed within the TVM (Stathopoulos et al., 2004).

We examined further the expression of FGF signaling components, and found that genes encoding both ligands for Htl, *ths* and *pyr*, are expressed in the TVM (Fig. 1J-J″). Ligand expression appears to be differentially regulated within the TVM, as *pyr* is only expressed early at stage 10 and 11, whereas *ths* expression spans stages 10-13 (supplementary material Fig. S2). By contrast, the *htl* gene encoding the FGFR is expressed in CVM cells (Fig. 1I) (Mandal et al., 2004) and we noticed its expression is also temporally regulated, as expression is not present until after CVM cells have initiated their migration (Fig. 1I; data not shown).

To investigate a role for this signaling pathway in regulating CVM cell migration, we assayed mutants that affect FGF signaling for effects on cell migration. Our results showed that CVM development is severely defective in the absence of FGF signaling (Fig. 2D-I). In the *Df(2R)BSC25* mutant, in which the linked *pyr* and *ths* genes are removed (Stathopoulos et al., 2004), CVM cells reach only half-way along their course when compared with the position obtained by wild-type CVM cells (compare Fig. 2H). This phenotype was comparable with that observed in *htl* mutants (Fig. 2E) (Mandal et al., 2004). Furthermore, the CVM cells in these mutants lost their close association with the TVM and exhibited an aberrant cell shape, as cells lost their ellipsoidal characteristics and nuclei were small and circular. In either *pyr* or *ths* single mutant embryos [*Df(2R)pyr36* and *Df(2R)ths238*, respectively (Kadam et al., 2009)], CVM phenotypes were also present but appeared less severe, with fewer cells exhibiting the altered morphology characteristic of both *htl* and *Df(2R)*BSC25 mutants (Fig. 2F,I compare with 2E,H). Longitudinal muscles were partially formed in the single mutants, whereas they were completely absent in *htl* mutants (Mandal et al., 2004) or *Df(2R)BSC25* mutants (data not shown). These results suggested that both ligands contribute to CVM cell migration.

Our next goal was to determine whether FGF signaling acts to influence CVM cells directly, possibly acting as a guidance factor, or instead might influence CVM cell migration indirectly through

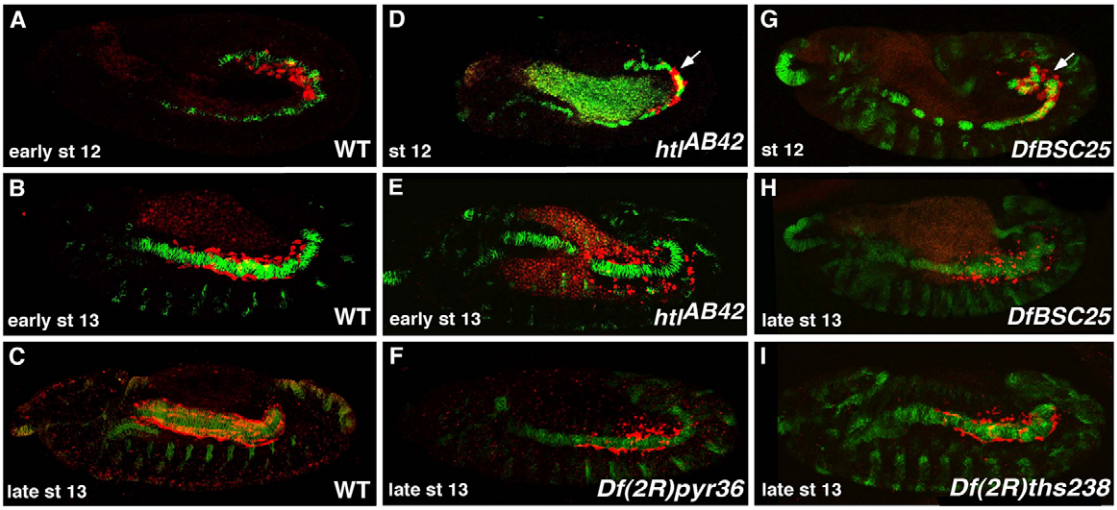

Fig. 2. CVM cell migration is aberrant in FGF mutants. Embryos are oriented with anterior towards the left and dorsal upwards. (**A-I**) Embryos of the following genotypes containing *croc-lacZ* were stained using anti-βgal antibody (red) to mark CVM and anti-FasIII antibody (green) to mark TVM: (A-C) wild type, (D,E) htl^{AB42} mutant embryos, (F) *Df(2R)*pyr36 (*pyr* single mutant), (G,H) *Df(2R)BSC25* (deficiency chromosome removing *pyr* and *ths*) and (I) *Df(2R)ths238* (*ths* single mutant). Embryos at stage 12 are depicted in A,D,G; embryos at stage 13 are depicted in B,C,E,F,H,I.

effect on another tissue (e.g. specification of TVM). FGF signaling is active pervasively throughout development in a number of different cell types, and, in particular, controls mesoderm spreading during gastrulation required for TVM specification (Frasch, 1995; Staehling-Hampton et al., 1994).

Gaps were identified at random positions within the TVM in the FGF mutants. However, we found that CVM cells were able to migrate past such gaps. At least at early stages in the migration process, an intact TVM is not required to support migration (Fig. 2D,G). Although anteriorly localized gaps sometimes correlated in position with cessation of migration (e.g. Fig. 2E), this defect was probably not causative as migration ceases at this point in mutants regardless (i.e. even when the TVM is intact; Fig. 2H).

Next, we specifically knocked down FGF signaling in the CVM and examined the effect on the migration of cells. To achieve this, we expressed a dominant-negative Htl receptor (UAS.DN-Htl) or dsRNA hairpin construct targeting *htl* transcripts (UAS.htl-RNAi) using the *G447.Gal4* driver, which supports expression of UAS-containing transgenes in CVM cells as well as an adjacent related population of cells, malphigian tubule (MT) precursors (Denholm et al., 2003; Georgias et al., 1997; Phelps and Brand, 1998). In both cases, CVM cell migration was clearly aberrant, with cells failing to reach the anterior section of the TVM and cell number appearing reduced, possibly owing to increased cell death (supplementary material Fig. S3). The phenotype was observed in 30-40% of embryos; such partial penetrance using transgene-mediate ectopic expression to reduce gene function is common (Dietzl et al., 2007). This result provided evidence that FGF signaling is required within migrating CVM cells directly, at least in part, to support their migration. Therefore, we subsequently conducted a directed set of experiments aimed at deciphering the role of FGF signaling within these cells.

FGF signaling supports CVM cell survival

As we had observed that CVM cell numbers are decreased and that cell nuclei appeared smaller and more circular from late stage 12 onwards in FGF mutants, we investigated whether cell death resulted in the absence of signaling. Using a standard TUNEL assay (e.g. Reim et al., 2003), we found that CVM cells undergo increased cell death in the *Df(2R)BSC25* mutant embryos as TUNEL-positive cells are identified by stage 13 (Fig. 3B,F) but not at earlier stages (Fig. 3E). By contrast, little to no cell death is associated with CVM cells present in wild-type embryos at any stage (Fig. 3A,D).

To test the idea that FGF signaling supports cell survival during CVM migration, we blocked CVM cell death in *Df(2R)BSC25* mutants by expressing the baculovirus anti-apoptotic p35 protein, a potent inhibitor of programmed cell death that inhibits *Drosophila* caspases (Huh et al., 2004). p35 was expressed within CVM cells of *Df(2R)BSC25* mutants using the *G447.Gal4* driver (Denholm et al., 2003; Georgias et al., 1997). Expression of p35 within CVM cells of *Df(2R)BSC25* mutant embryos kept cells alive. Specifically, cell number was similar to wild type, cell nuclei were of normal size and cells were once again closely associated with the TVM. However, CVM migration was not completely rescued in this background, for cells did not reach the anterior TVM position normally attainable by wild-type cells (Fig. 3C, compare with 3A). This result suggested that FGF signaling not only supports cell survival, as had been proposed previously (Mandal et al., 2004), but also likely regulates effective movement of CVM cells, allowing them to reach the most anterior position of the TVM.

FGFs regulate migration of two bilaterally symmetric clusters of CVM cells at early stages

In wild-type embryos, CVM cells originate as a single cluster and subsequently split into two bilaterally symmetric groups of ~30 cells on either side of the dorsal midline (Fig. 4A). We inferred from the examination of fixed sample that these two cell groups appeared to move in sync, with the leading cells of each group taking up equivalent positions along the length of the embryo at each timepoint examined (Fig. 4B,C).

By contrast, *htl* and *Df(2R)BSC25* mutants exhibited severe CVM cell migration defects affecting cell organization during the early stage of the migration process (Fig. 4G,E,H compare with 4D). Cells merged at the midline (‘merge’; Fig. 4E,G), and the two cell groups also moved out of sync (‘asynchrony’; Fig. 4H). Similar phenotypes were observed when either the UAS.DN-Htl or

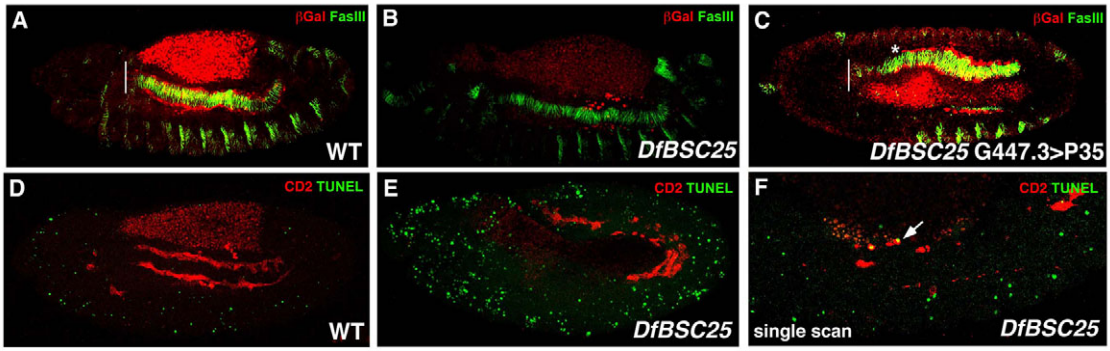

Fig. 3. FGF signaling supports CVM cell survival. Embryos are oriented with anterior towards the left and dorsal upwards. (**A-C**) Embryos containing the *croc-lacZ* reporter gene stained using anti-βgal (red) and anti-FasIII (green) to identify CVM and TVM cells, respectively. Wild-type (stage 13; A), *Df(2R)BSC25* (stage 13; B) and *Df(2R)BSC25* embryos expressing p35 via *G447.Gal4* driver (stage 13; C) are depicted. (C) Expression of the anti-apoptotic protein p35 rescues the morphology of CVM cells and allows cells to migrate anteriorly, but cells (asterisk) fail to reach the anterior-most position of the TVM (white line). (**D-F**) Cell death is observed in FGF mutants using the TUNEL assay. Wild-type embryo (i.e. *G447.Gal4 UAS-CD2*) of stage 13 (D) and *Df(2R)BSC25 G447.Gal4 UAS-CD2* embryos of stage 12 (E) and stage 13 (F) stained with anti-CD2 to detect CVM cells (red) and apoptosis using the TUNEL assay (green).

UAS.htl-RNAi constructs were expressed in the CVM using the *G447.Gal4* driver (Fig. 4F,I). Such convergence and/or loss of synchrony were rarely observed in wild-type embryos, whereas these phenotypes were commonly observed when FGF signaling was compromised, including in *pyr* and *ths* single mutants (Fig. 4J; see *Df(2R)pyr36* and *Df(2R)ths238*, respectively). These results suggested that FGF signaling within CVM cells directly regulates the movements of cells and, furthermore, involves activation of the Htl FGFR by both ligands Pyr and Ths.

Live in vivo imaging of CVM migration in wild-type and FGF mutant embryos

To provide further insights into how FGF signaling regulates CVM cell migration, we analyzed the migration of these cells by time-lapse live in vivo imaging using standard one-photon confocal microscopy and a fluorescent protein reporter constructed to label CVM cell nuclei (bHLH54F-H2A.Cherry). Embryos could be imaged for up to 3.5 hours with no discernable negative effect on viability under the imaging conditions used. CVM cell migration was visualized as early as stage 10 from either lateral or dorsal vantage points (supplementary material Movies 1 and 2, 'wild type', respectively).

To study the initial migratory sequence, we found movies taken from a dorsal vantage point were more informative (Fig. 5A; supplementary material Movie 2, 'wild type'). As suggested by the fixed tissue analysis, CVM cells split into two symmetric clusters that moved synchronously towards the anterior. Approximately 75 minutes later, the wild-type cells reached the anterior-most position of the dorsal half of the embryo and began their descent into ventral regions; at this point, each of the two CVM cell groups further subdivided, forming two rows within each migrating cluster. By ~100 minutes, half of the cells disappeared from the dorsal vantage point as they continued their migration toward the ventral half of the embryo and subsequently toward more anterior regions. In addition, live imaging confirmed that most of CVM cell migration observed was independent of GBR, as retraction initiated after the CVM cells had clearly migrated a substantial distance.

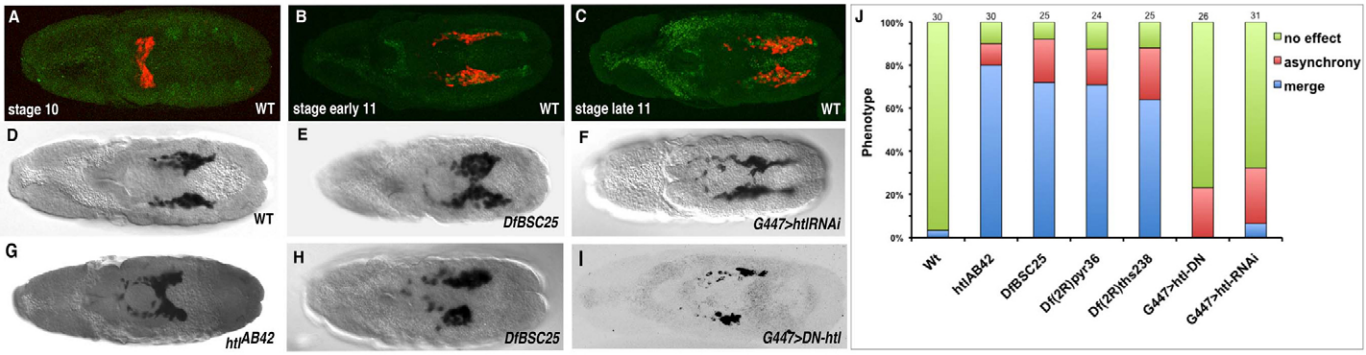

Fig. 4. FGF mutants exhibit early CVM cell migration defects. (A-I) Dorsal views of embryos containing the *croc-lacZ* reporter, oriented with anterior towards the left. (**A-C**) Embryos were co-stained using anti-βgal (red) and anti-Biniou antibody (green) to identify CVM cells and presumptive TVM tissue early in CVM cell migration. (A) Bilateral clusters form; (B) cell groups initiate movement towards the embryonic anterior in a synchronous fashion; and (C) eventually move from dorsal to ventral regions of the embryo, out of view. (**D-I**) Embryos containing the *croc-lacZ* reporter were stained with anti-βgal antibody and stained to mark CVM cells at stage 11. Wild-type (WT; D); *Df(2R)BSC25*, *ths* and *pyr* 'double mutant' (E,H); htl^{AB42} mutant (G); embryos expressing a *htl* RNAi UAS-hairpin construct in the CVM cells through *G447.Gal4*-mediated expression (F); and embryos expressing dominant-negative Htl in the CVM cells through *G447.Gal4*-mediated expression of UAS-*htl.dn* (I). (**J**) Phenotypic categorization for each FGF mutant background within three categories: no effect on migration (green), asynchronous migration of the two cell groups (red), or merging of the two CVM cell clusters (blue). '*n*' is defined as the number of embryos scored for each of the indicated genotypes above each bar.

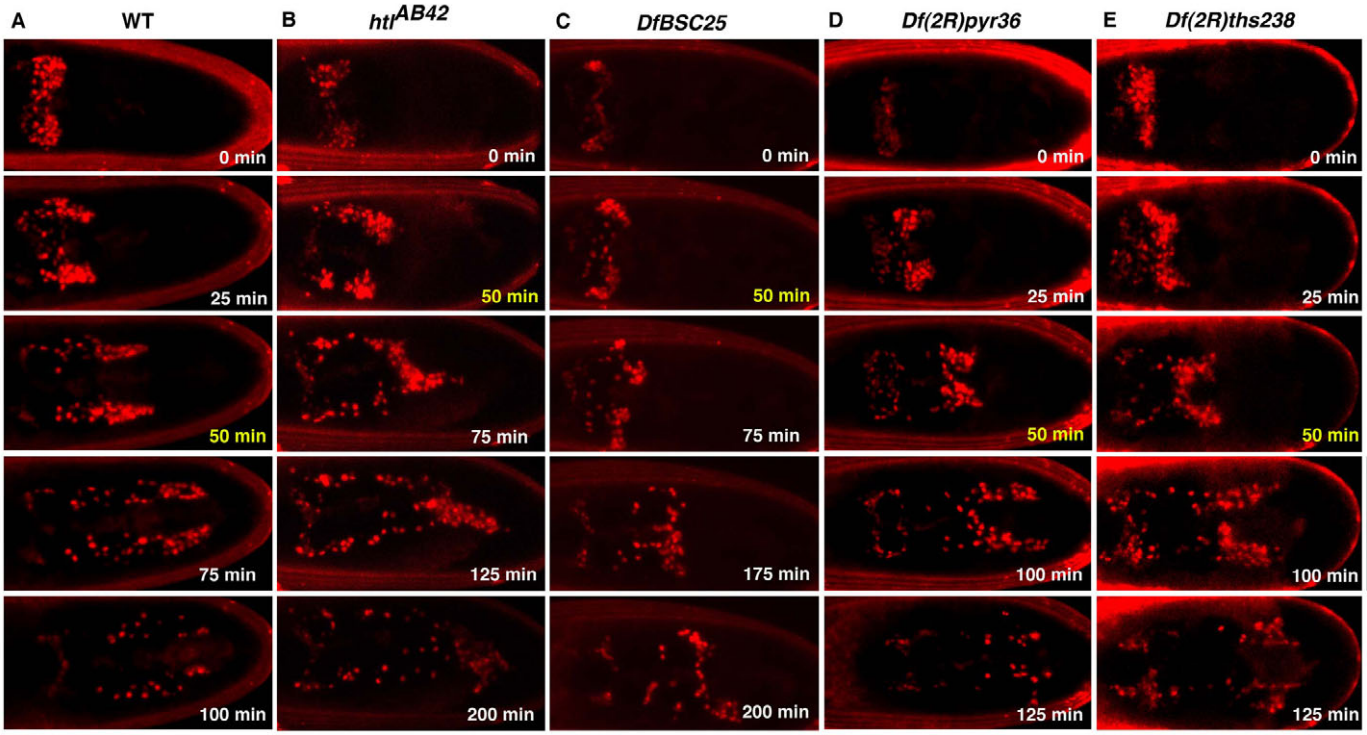

Fig. 5. Live in vivo imaging of CVM migration in wild-type and mutant embryos. Dorsal views of embryos oriented with anterior towards the left. (**A-E**) Stills from ~3 hour movies of CVM cells imaged within embryos containing the bHLH54F-H2A-mCherry reporter of the following genetic backgrounds: (A) wild type; (B) *htl*^{AB42}; (C) *DfBSC25*; (D) *Df(2Rpyr36*; and (E) *Df(2R)ths238*. Selective stills are shown at representative times throughout the course of the migration are shown. For example, at 50 minutes (yellow label), CVM cells within wild-type (A) and single mutant (D,E) embryos are actively migrating, whereas in *htl*^{AB42} (B) and *DfBSC25* (C) mutant embryos the CVM cells appear stalled.

Live imaging of CVM cells in *htl* FGFR mutants and *Df(2R)BSC25* FGF double mutants confirmed their migration was aberrant (Fig. 5B,C; supplementary material Movie 2, '*htl*' and '*DfBSC25*'). In the mutant backgrounds, two equivalent groups of cells were formed and migration initiated, but appeared to stall soon thereafter. By 50 minutes, migrating CVM cells had moved only a short distance towards the anterior in these FGF mutants, and cell movements were clearly misdirected and oriented toward the midline; merging of the two clusters was observed. Eventually, CVM cells migrated toward the anterior direction albeit at a reduced speed. More than double the amount of time was required for cells to migrate to ventral regions (and subsequently move out of frame) in these mutants compared with wild type.

Loss of either *pyr* or *ths* caused an intermediate effect: CVM cell migration was slower than in wild-type embryos but not as slow as that observed in the *Df(2R)*BSC25 mutant embryos (Fig. 5D,E compare with A,C; supplementary material Movie 2, '*pyr*' and '*ths*'). As in *Df(2R)*BSC25 mutant embryos, a fraction of CVM cells also appeared misdirected in the *pyr* or *ths* single mutant embryos (i.e. exhibited a 'merge' phenotype).

Tracking analysis reveals mixing occurs and bilateral symmetry is lost

We used a cell tracking analysis, aided by Imaris software, to better characterize CVM cell migration as it allowed us to analyze individual cell behaviors relative to group dynamics (Fig. 6; supplementary material Movie 3). In *Df(2R)BSC25* mutants, cell tracking analysis confirmed that cells from one side crossed over to the other side, which was never observed in wild type (Fig. 6A, compare with 6B; supplementary material Movie 3 'wild type' versus 'DfBSC25'). Effectively, cells from one group joined the other migrating collective, resulting in a loss of bilateral symmetry. In *htl* mutant embryos, the merging phenotype of the two CVM clusters was even more severe (Fig. 6C; supplementary material Movie 3 '*htl*'). In the *Df(2R)BSC25* mutants, after mixing the two clusters sometimes resolved, whereas, in the *htl* mutant, cells stayed clumped near the midline.

FGFs provide chemoattractive cues to direct CVM cell migration

We hypothesized that the FGF ligands provide an attractive signal that influences CVM migration, and that their expression within the TVM keeps cells on track during the course of migration. In order to investigate whether FGFs act as chemoattractants, we used different Gal4 drivers to express ligands in a temporally and spatially controlled manner within mutant embryos devoid of endogenous Pyr and Ths FGF ligand [i.e. within a deficiency mutant that deletes both *pyr* and *ths* genes as well as several other genes, *Df(2R)BSC25* (Stathopoulos et al., 2004)].

First, *single minded* (*sim*).*Gal4* (Xiao et al., 1996) was used to drive expression in the ventral midline of *Df(2R)BSC25* mutant embryos, in order to determine whether FGFs could attract the CVM cells from a relatively close ectopic position (i.e. the proximity of the midline from the CVM cells at the start of their migration is ~50 μm). When either *ths* or *pyr* were expressed in the midline of *Df(2R)BSC25* mutant embryos using *sim.Gal4*, the CVM cells were redirected towards the source of ectopic FGF expression (Fig. 7F,G, compare with 7B; Fig. 7H, compare with

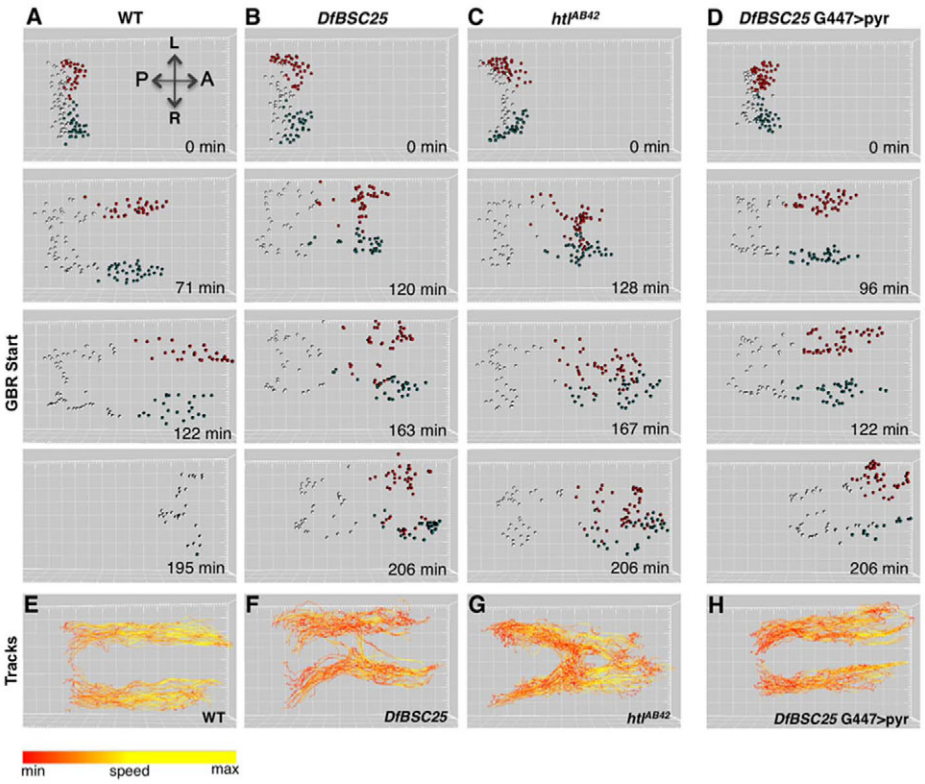

Fig. 6. Cell tracking analysis reveals CVM cells cross over the midline in the absence of FGF signaling. Dorsal view of embryos oriented with anterior towards the left. Manual tracking analysis was conducted on movies obtained through live in vivo imaging of CVM cell migration using a bHLH54F-H2A.mCherry reporter (Movie 3). (**A-D**) This analysis was carried out on wild type (A), and on *Df(2R)BSC25* (B), *htl*^{AB42} (C) and *Df(2R)BSC25 G447.Gal4 UAS.pyr* mutant backgrounds (D). Red cells indicate CVM cells initially located on the right side of the embryo; blue cells indicate CVM cells initially located on the left side of the embryo; and gray cells indicate malphigian tubule (MT) precursor cells, which are a distinct group of cells that function to specify the renal tubules. GBR (third row) starts ~120 minutes after cluster separation in wild-type (A) and *Df(2R)BSC25 G447.Gal4 UAS.pyr* (D) embryos, but not until ~160-170 minutes in FGF mutants: *Df(2R)BSC25* (B) and *htl*^{AB42} (C). (**E-H**) Tracks representative of the paths taken by CVM cells of wild-type (E), *htl*^{AB42} mutant (G), Df*(2R)BSC25* mutant (F) and *Df(2R)BSC25 G447>pyr* mutant (H) backgrounds. The tracks represent the movement of CVM specifically, as tracks for MT precursor cells were excluded from view. The key refers to instantaneous speed of cells, with red representing the slowest speed and yellow the fastest speed.

7D). Moreover, CVM cells that moved towards the midline maintained the normal morphology, suggesting that these cells survived.

By comparison, ectopic expression of *ths* or *pyr* at a distance in *Df(2R)BSC25* mutant embryos, within the salivary glands via *forkhead* (*fkh*).*Gal4* (Henderson and Andrew, 2000), also supported CVM cell migration and partial cell survival (Fig. 7J-L, compare with Fig. 2H). However, this long-distance FGF action did not fully rescue, as CVM cells never reached the anterior-most position as in wild type (Fig. 7J,K compare with 7C). We propose that this relates to the finding that their migration was misdirected at early stages (Fig. 7L, compare with 7D); as some of their movements were off course, this probably stalled their anteriorly directed progress.

Rescue experiments by ectopic expression of ligands

Having demonstrated that the FGF ligands could function as chemoattractants to attract CVM cells to an ectopic location, we investigated whether ligands normally function as chemoattractants to support association of CVM cells with the TVM. To this end, we examined whether presentation of the ligands within the TVM might serve to rescue the *DfBSC25* mutant phenotype. Targeted expression of either *ths* or *pyr* FGF ligand within the TVM was accomplished using the *bagpipe* (*bap*).*Gal4* driver (Azpiazu and Frasch, 1993) (supplementary material Fig. S4A) but supported only a partial rescue: cell survival increased and cells migrated farther, but in both cases cells failed to reach the anterior-most position of the TVM normally attainable in wild type (supplementary material Fig. S4A). Early rescue was not supported, with cells continuing to 'merge' at the midline in early stages, suggesting that the *bap.Gal4* driver may not support expression of ligands early enough and/or that expression of both ligands is required for full rescue.

If exogenous FGF ligand is functioning as a guidance cue to the migrating CVM cells, we hypothesized that overexpression of FGF ligands in the migrating CVM cells themselves may prevent these cells from aligning with the TVM. To test this idea, we ectopically expressed *pyr* or *ths* in CVM cells using the *G447.Gal4* driver (supplementary material Fig. S4C; data not shown). Unexpectedly, expression of *pyr* or *ths* in the CVM rescued the early crossing-over phenotype associated with the *Df(2R)BSC25* mutant background: cells migrated effectively as two groups in proximity to the TVM tracks (supplementary material Fig. S4C). We confirmed this result through tracking analysis of live in vivo imaging studies; no 'merging' phenotype in the mutant background was observed upon *G447.Gal4*-mediated expression of *pyr* (Fig. 6D,H, compare with 6B,F) or *ths* (in four out of five embryos; data not shown).

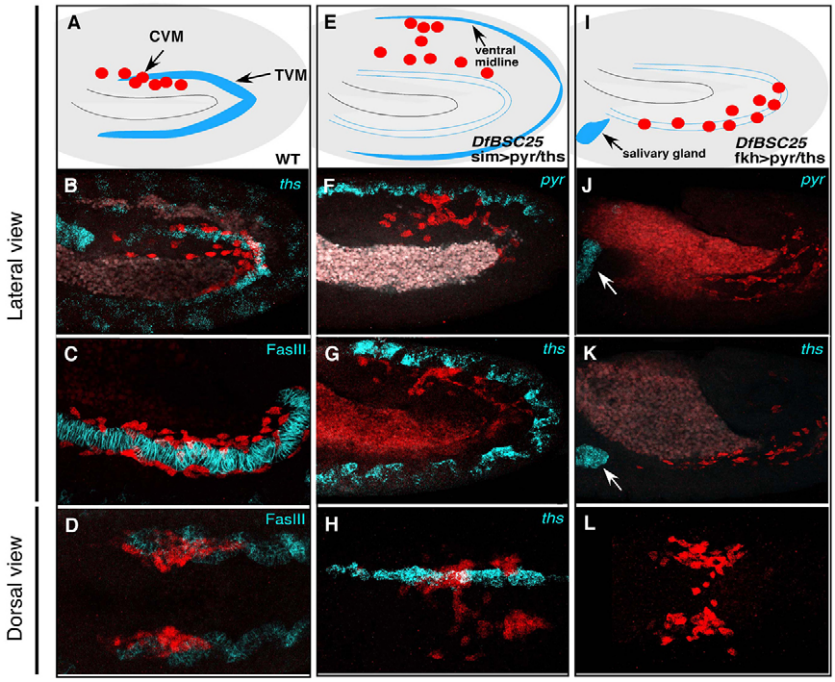

Fig. 7. FGFs function in a chemoattractive manner to direct CVM cell movement. Embryos oriented with anterior towards the leftor lateral views are shown as indicated. (**A**,**E**,**I**) Schematics are based on lateral views of a wild-type embryo with native expression of ligands (A), or of *DfBSC25* mutant embryos devoid of endogenous ligand in which either the *sim.Gal4* driver (E) or *fkh.Gal4* driver (I) is used to support ectopic expression of ligand at the ventral midline or salivary gland, respectively. CVM cells are represented by red circles and the domain of endogenous (A) or ectopic expression (E,I) of ligands is marked in blue. (**B-D**,**F-H**,**J-L**) Lateral (B,F,G, late stage 11; C,J,K, early stage 13) or dorsal (D,H,L, stage 11) views of stained embryos are shown. All embryos contain the *croc-lacZ* reporter gene and anti-βgal antibody was used to detect CVM cells (red). Anti-FasIII antibody was used to identify TVM (blue) in C,D, whereas riboprobes to either *pyr* or *ths* transcripts (blue, as indicated) were used to detect either endogenous expression (B, *ths*) or the domain of ectopic expression supported by *sim.Gal4* (F, *pyr*; G, *ths*; H, *ths*) or *fkh.Gal4* (J, *pyr*; K, *ths*).

Ligands in combination have different effects when presented individually

As our genetic analysis and ectopic expression experiments suggested that both Pyr and Ths ligands influence CVM cell migration, we next examined how ligand levels and/or combinatorial interactions between ligands might influence this process. Expression of a single copy of either *pyr* or *ths* at the midline in the *Df(2R)BSC25* mutant background using the *sim.Gal4* driver recruits a subset of CVM cells, without much effect on the majority of cells, which remain associated with the TVM as two migrating cell clusters (Fig. 8F,G, compare with 8A; supplementary material Movie 4 '1×pyr' and '1×ths' compare with Movie 2 'wild type'); similar to fixed analyses (Fig. 7E-H). Expression of two copies of either gene was able to recruit even more CVM cells to the midline (Fig. 8D,E; supplementary material Movie 4 '2×pyr' and '2×ths'), with 2×ths exhibiting a slightly stronger influence. Despite the ectopic expression of ligands at the midline, most CVM cells continued to move towards the anterior.

By contrast, ectopic expression of one copy of each gene together (1×pyr + 1×ths) resulted in a surprising output: CVM cell migration stalled (Fig. 8B; supplementary material Movie 4 '1×pyr+1×ths'). Cells moved towards the anterior only with GBR, suggesting movement was passive. However, a few cells at the leading edge did migrate away from the group towards the anterior (supplementary material Movie 4 '1×ths+1×pyr', arrows).

Furthermore, ectopic *pyr* and/or *ths* expression was able to redirect CVM cell migration to the ventral midline only in a homozygous *Df(2R)BSC25*, *pyr* or *ths* mutant background (Fig. 8B,D-I), but not when endogenous sources of both ligands were present. For example, within a *Df(2R)BSC25* heterozygous background, CVM cell migration appeared normal and cells were not observed to migrate off track despite ectopic expression of both ligands at the midline (Fig. 8C and Movie 5). However, CVM cells could be redirected to the midline in *pyr* and *ths* single mutants, suggesting that endogenous expression of both ligands is required to keep cells from being misdirected (Fig. 8H,I; data not shown). Collectively, these results demonstrate that when endogenous expression of both *pyr* and *ths* is intact, it serves as a very effective guidance cue for CVM cell migration; in this case, ectopic sources of the ligand presumably cannot compete and therefore fail to misdirect cells to the midline.

DISCUSSION

FGF signaling promotes anteriorly directed movement of CVM cells along the TVM

Our results show that FGF signaling through Htl, Pyr and Ths is required to limit lateral movement of CVM cells as they move anteriorly along the TVM. An unanswered question is how Pyr and Ths ligands, which appear isotropically expressed along the entire length of the TVM, could support anteriorly directed movement. We suggest that as cells move towards the anterior, they contribute to establishment of the FGF activity gradient, as has been proposed for other isotropically expressed cell migration guidance cues (Streichan et al., 2011), and could explain how G447-Gal4-mediated expression of ligands within the CVM cells supports rescue.

It is thought that FGF ligands interact with the FGFR as a heterotrimeric complex with heparan sulfate proteoglycans (HSPGs) (Knox et al., 2011; Lin et al., 1999). Therefore, another possibility is that an HSPG, or other similar molecule necessary to promote effective FGF-FGFR interactions, is differentially expressed within the TVM and contributes to anteriorly directed movement of CVM cells. For example, our data show that re-routing of CVM cells to an ectopic location is only possible when endogenous expression of at least one ligand is absent; we suggest this may result from additional influence on receptor-ligand interactions by third-party molecules such as HSPGs expressed in the TVM, which make ligands more potent chemoattractants at this position. Alternatively, it is also possible that ligands are more efficiently processed when expressed at the TVM.

In addition, our results show that the *htl* mutant phenotype, as identified by tracking analysis, is more severe than loss of both ligands, *Df(2R)BSC25*. In *htl* mutants, CVM cells converge at the midline whereas in the absence of both ligands, only a subset of cells crossover. Our data suggest that the Htl receptor may retain some limited activity, even in the absence of Pyr and Ths ligands.

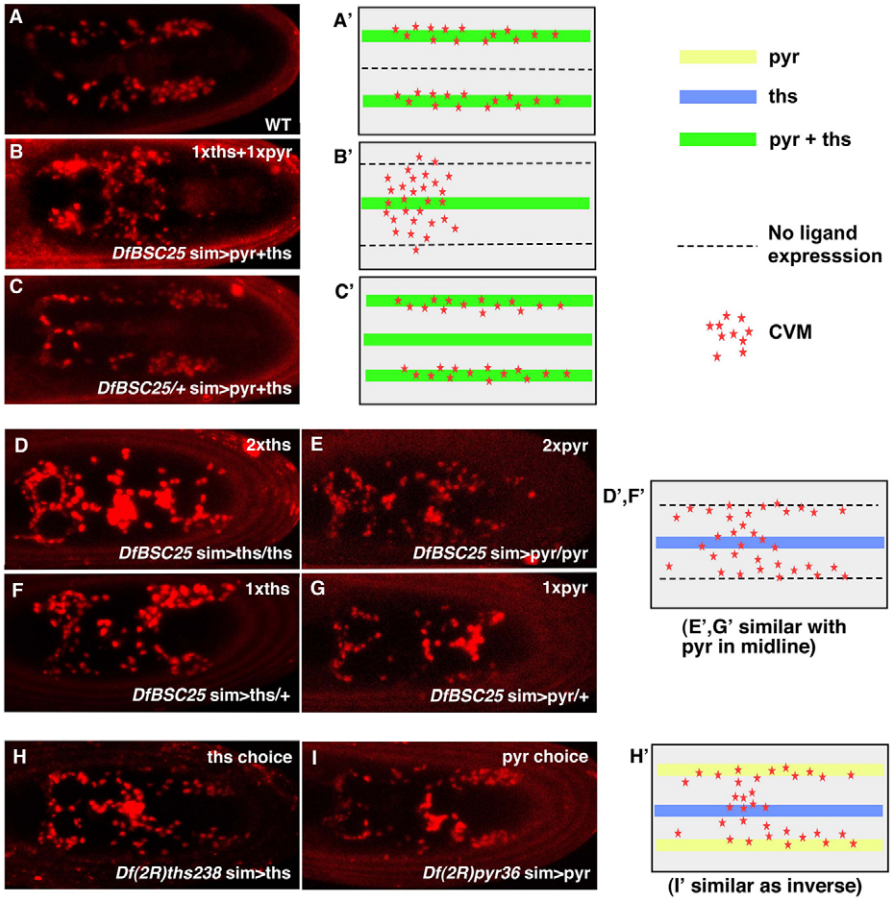

Fig. 8. Expression of ligands either individually or in combination has different effects on CVM cell migration. Shown are dorsal views of embryos oriented with the anterior towards the left. The *sim.Gal4* driver was used to drive ectopic expression of *UAS.ths* and/or *UAS.pyr* at the ventral midline within wild-type or mutant embryos as indicated. Representative stills from movies taken of embryos containing the bHLH54F-H2A.Cherry reporter of the following genotypes: (**A**) wild-type; (**B**) *Df(2R)BSC25* homozygous mutant embryos ectopically expressing *pyr* and *ths* at the ventral midline through *sim.Gal4*-mediated ectopic expression; (**C**) *Df(2R)BSC25*/+ heterozygous mutant embryos expressing both *pyr* and *ths* via *sim.Gal4*; (**D**,**F**) *Df(2R)BSC25* mutant genetic background containing either two (D) or one (F) copy of *ths*; (**E**,**G**) *Df(2R)BSC25* mutant genetic background containing either two (E) or one (G) copy of *pyr*; (**H**) *ths* single mutant (i.e. *pyr* endogenous expression intact) ectopically expressing *ths* at the midline; or (**I**) *pyr* single mutant (i.e. *ths* endogenous expression intact) ectopically expressing *pyr* at the midline. (**A′-D′,″,H′**) Schematics showing where *pyr* and/or *ths* are expressed in the TVM and/or midline and the effect on CVM cell migration.

Ligand synergy at the level of receptor binding or intracellular response?

Although ectopic expression of ligands individually appears to clearly redirect cells to the midline, expression of both ligands together supported a surprising result. Co-expression of both ligands resulted in a distinct phenotype, in which CVM cell migration was severely stalled. The finding that ectopic co-expression of *pyr* and *ths* together causes such a phenotype could be due to several reasons. First, it is possible that both ligands together act as a more potent chemoattractant and/or elicit a strong response to FGF, which makes cells unable to respond to other signals; for example, we propose that another uncharacterized signal exists, which is capable of driving anterior movement of cells even in the FGF mutant background. Alternatively, or in addition, it is possible that the combination of both ligands impacts the adhesive nature of the migrating cell collective; increased cell adhesivity may cause CVM cells to adhere more strongly to each other and thus inhibit their mobility. Interestingly, though the majority of cells are immobile, a few cells that break away from the collective appear to migrate towards the anterior just fine, suggesting that cells, when dissociated from the group, can sense directional signals (supplementary material Movie 4, '1×ths+1×pyr', arrows).

Several possibilities exist for how these ligands may function coordinately. It is possible that Pyr and Ths function as a heterodimeric complex, which acts differently from each homodimer. Alternatively, the ligands may promote activation of independent signaling pathways, which synergize when both ligands are present. Future studies aimed at biochemical characterization of ligand-receptor interactions and the identification of active intracellular signaling pathways should shed light on the underlying molecular mechanisms.

CVM cell migration is probably guided by multiple directional cues

During the early stage of CVM cell migration, even in the absence of FGF signaling, cells move forward towards the anterior. Eventually, they become misdirected, resulting in the two cell groups converging at the midline, but the two groups continue to move towards the anterior albeit at a slower rate. Furthermore, we observed that *htl* expression is not observed until after CVM cells have started migrating, which suggests that another unidentified guidance cue also influences CVM cell migration at the very start of their migration, before FGF signaling plays a role. In addition, although not required for cell movement, GBR may provide physical force that helps CVM cells round the turn from dorsal to ventral regions of the embryo to contribute to full migration. As the full course of the migration takes ~6 hours, it is likely that a number of guidance cues contribute to effective CVM migration.

Besides supporting a role in guiding directed movement of cells, FGF signaling may be required to fulfil other functions during the course of migration. FGF signaling influences CVM cell survival, and may also regulate cell proliferation. While cell death may occur as a checkpoint mechanism to deal with cells veering off course in the absence of FGF-mediated cell guidance, FGF signaling may also directly impact cell survival. Furthermore, in wild-type embryos, the CVM cells divide three times during the course of their migration (S.K., unpublished observations). Ectopic expression of ligands leads

to an increase in the number of cells present in dorsal regions, but whether this relates to an increase in proliferation or occurs because the movement of cells is slowed remains to be determined. Future studies aimed at analysis of the full course of the migration will provide additional answers and, although these experiments are not yet technically possible, advances in microscopy make this a promising avenue for future research.

Acknowledgements
We thank Leslie Dunipace, Alphan Altinok and Sarah Wadsworth for excellent technical assistance; Manfred Frasch and Mayra Garcia for helpful discussions; and Marianne Bronner and members of the Stathopoulos laboratory, especially Young Bae, for comments on the manuscript. In addition, we are grateful to Rolf Reuter for sharing fly strains, providing the schematic shown in Fig. 1 and supporting S.K.'s preliminary studies of CVM cell migration (parts of supplementary material Fig. S1 and Fig. S2).

Funding
This work was funded by a grant from the National Institute of General Medical Sciences (NIGMS) [R01GM078542 to A.S.]. Deposited in PMC for release after 12 months.

Competing interests statement
The authors declare no competing financial interests.

Author contributions
S.K. and A.S. designed the experiments; S.K. conducted all the experiments except the manual tracking in Fig. 6, which was carried out by S.G.; S.K. and A.S. analyzed the data and wrote the manuscript.

Supplementary material
Supplementary material available online at
http://dev.biologists.org/lookup/suppl/doi:10.1242/dev.068791/-/DC1

References
Aman, A. and Piotrowski, T. (2010). Cell migration during morphogenesis. *Dev. Biol.* **341**, 20-33.
Azpiazu, N. and Frasch, M. (1993). tinman and bagpipe: two homeo box genes that determine cell fates in the dorsal mesoderm of *Drosophila*. *Genes Dev.* **7**, 1325-1340.
Beiman, M., Shilo, B. Z. and Volk, T. (1996). Heartless, a *Drosophila* FGF receptor homolog, is essential for cell migration and establishment of several mesodermal lineages. *Genes Dev.* **10**, 2993-3002.
Denholm, B., Sudarsan, V., Pasalodos-Sanchez, S., Artero, R., Lawrence, P., Maddrell, S., Baylies, M. and Skaer, H. (2003). Dual origin of the renal tubules in *Drosophila*: mesodermal cells integrate and polarize to establish secretory function. *Curr. Biol.* **13**, 1052-1057.
Dietzl, G., Chen, D., Schnorrer, F., Su, K. C., Barinova, Y., Fellner, M., Gasser, B., Kinsey, K., Oppel, S., Scheiblauer, S. et al. (2007). A genome-wide transgenic RNAi library for conditional gene inactivation in *Drosophila*. *Nature* **448**, 151-156.
Franzdottir, S. R., Engelen, D., Yuva-Aydemir, Y., Schmidt, I., Aho, A. and Klambt, C. (2009). Switch in FGF signalling initiates glial differentiation in the *Drosophila* eye. *Nature* **460**, 758-761.
Frasch, M. (1995). Induction of visceral and cardiac mesoderm by ectodermal Dpp in the early *Drosophila* embryo. *Nature* **374**, 464-467.
Friedl, P. and Gilmour, D. (2009). Collective cell migration in morphogenesis, regeneration and cancer. *Nat. Rev. Mol. Cell. Biol.* **10**, 445-457.
Georgias, C., Wasser, M. and Hinz, U. (1997). A basic-helix-loop-helix protein expressed in precursors of *Drosophila* longitudinal visceral muscles. *Mech. Dev.* **69**, 115-124.
Gisselbrecht, S., Skeath, J. B., Doe, C. Q. and Michelson, A. M. (1996). heartless encodes a fibroblast growth factor receptor (DFR1/DFGF-R2) involved in the directional migration of early mesodermal cells in the *Drosophila* embryo. *Genes Dev.* **10**, 3003-3017.
Goldman-Levi, R., Miller, C., Greenberg, G., Gabai, E. and Zak, N. B. (1996). Cellular pathways acting along the germband and in the amnioserosa may participate in germband retraction of the *Drosophila melanogaster* embryo. *Int. J. Dev. Biol.* **40**, 1043-1051.
Hacker, U., Kaufmann, E., Hartmann, C., Jurgens, G., Knochel, W. and Jackle, H. (1995). The *Drosophila* fork head domain protein crocodile is required for the establishment of head structures. *EMBO J.* **14**, 5306-5317.
Henderson, K. D. and Andrew, D. J. (2000). Regulation and function of Scr, exd, and hth in the *Drosophila* salivary gland. *Dev. Biol.* 362-374.
Huh, J. R., Guo, M. and Hay, B. A. (2004). Compensatory proliferation induced by cell death in the *Drosophila* wing disc requires activity of the apical cell death caspase Dronc in a nonapoptotic role. *Curr. Biol.* **14**, 1262-1266.
Ismat, A., Schaub, C., Reim, I., Kirchner, K., Schultheis, D. and Frasch, M. (2010). HLH54F is required for the specification and migration of longitudinal gut muscle founders from the caudal mesoderm of *Drosophila*. *Development* **137**, 3107-3117.
Jakobsen, J. S., Braun, M., Astorga, J., Gustafson, E. H., Sandmann, T., Karzynski, M., Carlsson, P. and Furlong, E. E. (2007). Temporal ChIP-on-chip reveals Biniou as a universal regulator of the visceral muscle transcriptional network. *Genes Dev.* **21**, 2448-2460.
Jiang, J., Kosman, D., Ip, Y. T. and Levine, M. (1991). The dorsal morphogen gradient regulates the mesoderm determinant twist in early *Drosophila* embryos. *Genes Dev.* **5**, 1881-1891.
Kadam, S., McMahon, A., Tzou, P. and Stathopoulos, A. (2009). FGF ligands in *Drosophila* have distinct activities required to support cell migration and differentiation. *Development* **136**, 739-747.
Keller, R. (2005). Cell migration during gastrulation. *Curr. Opin. Cell Biol.* **17**, 533-541.
Klingseisen, A., Clark, I. B., Gryzik, T. and Muller, H. A. (2009). Differential and overlapping functions of two closely related Drosophila FGF8-like growth factors in mesoderm development. *Development* **136**, 2393-2402.
Knox, J., Moyer, K., Yacoub, N., Soldaat, C., Komosa, M., Vassilieva, K., Wilk, R., Hu, J., Vasquez Pas, L. D., Syed, Q. et al. (2011). Syndecan contributes to heart cell specification and lumen formation during *Drosophila* cardiogenesis. *Dev. Biol.* **356**, 279-290.
Kosman, D., Mizutani, C. M., Lemons, D., Cox, W. G., McGinnis, W. and Bier, E. (2004). Multiplex detection of RNA expression in *Drosophila* embryos. *Science* **305**, 846.
Kunwar, P. S., Siekhaus, D. E. and Lehmann, R. (2006). In vivo migration: a germ cell perspective. *Annu. Rev. Cell Dev. Biol.* **22**, 237-265.
Kusch, T. and Reuter, R. (1999). Functions for Drosophila brachyenteron and forkhead in mesoderm specification and cell signalling. *Development* **126**, 3991-4003.
Le T., Liang, Z., Patel, H., Yu, M. H., Sivasubramaniam, G., Slovitt, M., Tanentzapf, G., Mohanty, N., Paul, S. M., Wu, V. M. and Beitel, G. J. (2006). A new family of Drosophila balancer chromosomes with a w- dfd-GMR yellow fluorescent protein marker. *Genetics* **174**, 2255-2257.
Lin, X., Buff, E. M., Perrimon, N. and Michelson, A. M. (1999). Heparan sulfate proteoglycans are essential for FGF receptor signaling during Drosophila embryonic development. *Development* **126**, 3715-3723.
Mandal, L., Dumstrei, K. and Hartenstein, V. (2004). Role of FGFR signaling in the morphogenesis of the *Drosophila* visceral musculature. *Dev. Dyn.* **231**, 342-348.
McMahon, A., Reeves, G. T., Supatto, W. and Stathopoulos, A. (2010). Mesoderm migration in *Drosophila* is a multi-step process requiring FGF signaling and integrin activity. *Development* **137**, 2167-2175.
Michelson, A. M., Gisselbrecht, S., Zhou, Y., Baek, K. H. and Buff, E. M. (1998). Dual functions of the heartless fibroblast growth factor receptor in development of the *Drosophila* embryonic mesoderm. *Dev. Genet.* **22**, 212-229.
Montell, D. J. (2006). The social lives of migrating cells in *Drosophila*. *Curr. Opin. Genet. Dev.* **16**, 374-383.
Parent, C. A. and Devreotes, P. N. (1999). A cell's sense of direction. *Science* **284**, 765-770.
Phelps, C. B. and Brand, A. H. (1998). Ectopic gene expression in *Drosophila* using GAL4 system. *Methods* **14**, 367-379.
Plotnikov, A. N., Hubbard, S. R., Schlessinger, J. and Mohammadi, M. (2000). Crystal structures of two FGF-FGFR complexes reveal the determinants of ligand-receptor specificity. *Cell* **101**, 413-424.
Reim, I., Lee, H. H. and Frasch, M. (2003). The T-box-encoding Dorsocross genes function in amnioserosa development and the patterning of the dorsolateral germ band downstream of Dpp. *Development* **130**, 3187-3204.
Ridley, A. J., Schwartz, M. A., Burridge, K., Firtel, R. A., Ginsberg, M. H., Borisy, G., Parsons, J. T. and Horwitz, A. R. (2003). Cell migration: integrating signals from front to back. *Science* **302**, 1704-1709.
Rorth, P. (2011). Whence directionality: guidance mechanisms in solitary and collective cell migration. *Dev. Cell* **20**, 9-18.
Staehling-Hampton, K., Hoffmann, F. M., Baylies, M. K., Rushton, E. and Bate, M. (1994). dpp induces mesodermal gene expression in *Drosophila*. *Nature* **372**, 783-786.
Stathopoulos, A., Tam, B., Ronshaugen, M., Frasch, M. and Levine, M. (2004). pyramus and thisbe: FGF genes that pattern the mesoderm of *Drosophila* embryos. *Genes Dev.* **18**, 687-699.
Streichan, S. J., Valentin, G., Gilmour, D. and Hufnagel, L. (2011). Collective cell migration guided by dynamically maintained gradients. *Phys. Biol.* **8**, 045004.
Tulin, S. and Stathopoulos, A. (2010). Extending the family table: Insights from beyond vertebrates into the regulation of embryonic development by FGFs. *Birth Defects Res. C Embryo Today* **90**, 214-227.
Xiao, H., Hrdlicka, L. A. and Nambu, J. R. (1996). Alternate functions of the single-minded and rhomboid genes in development of the Drosophila ventral neuroectoderm. *Mech. Dev.* **58**, 65-74.
Zhang, X., Ibrahimi, O. A., Olsen, S. K., Umemori, H., Mohammadi, M. and Ornitz, D. M. (2006). Receptor specificity of the fibroblast growth factor family. The complete mammalian FGF family. *J. Biol. Chem.* **281**, 15694-15700.